Molecular Interactions in Paracrystals of a Fragment Corresponding to the α-Helical Coiled-Coil Rod Portion of Glial Fibrillary Acidic Protein: Evidence for an Antiparallel Packing of Molecules and Polymorphism Related to Intermediate Filament Structure

Murray Stewart, Roy A. Quinlan, and Robert D. Moir

Medical Research Council Laboratory of Molecular Biology, Cambridge CB2 2QH, England

Abstract. We have expressed in *Escherichia coli* a fragment of c-DNA that broadly corresponds to the α-helical coiled-coil rod section of glial fibrillary acidic protein (GFAP) and have used the resultant protein to prepare paracrystals in which molecular interactions can be investigated. An engineered fragment of mouse GFAP c-DNA was inserted into a modified version of the *E. coli* expression vector pLcII, from which large quantities of a λ cII-GFAP rod fusion protein were prepared. A protein fragment corresponding to the GFAP rod was then obtained by proteolysis with thrombin. Paracrystals of this material were produced using divalent cations (Mg, Ca, Ba) in the presence of a chaotrophic agent such as thiocyanate. These paracrystals showed a number of polymorphic patterns that were based on a fundamental pattern that had dyad symmetry and an axial repeat of 57 nm. Analysis of both positive and negative staining patterns showed that this fundamental pattern was consistent with a unit cell containing two 48-nm-long molecules in an antiparallel arrangement with their NH_2 termini overlapping by $\sim$34 nm. More complicated patterns were produced by stacking the fundamental pattern with staggers of approximately 1/5, 2/5, and 1/2 the axial repeat. The molecular packing the unit cell was consistent with a range of solution studies on intermediate filaments that have indicated that a molecular dimer (i.e., a tetramer containing four chains or two coiled-coil molecules) is an intermediate in filament assembly. Moreover, these paracrystals allow the molecular interactions involved in the tetramer to be investigated in some detail.

INTERMEDIATE filaments are a widely distributed class of cytoskeletal components that perform a number of key structural roles in eukaryotic cells and are also thought to be an important determinant of cytoplasmic organization (see references 34, 38, 49–52 for reviews). The proteins from which intermediate filaments are constituted are members of a large multigene family of which six general tissue-specific classes have been identified (11, 50): keratins (expressed in epithelial cells), vimentin (expressed in cells of mesenchymal origin), desmin (expressed in muscle cells), neurofilament proteins (expressed in nerve cells), glial fibrillary acidic protein (GFAP[1]; expressed in glial cells) and finally the lamins that are components of the fibrous lamina that underlies the nuclear envelope of most eukaryotic cells.

Intermediate filament proteins form two-chain molecules which all have a similar basic architecture (see Fig. 1) with

a central rod-like domain $\sim$310 residues long, which is thought to have an α-helical coiled-coil conformation, and globular domains at both NH_2 and COOH terminii (11, 19, 20, 49, 50). As illustrated in Fig. 1, the central rod domain can be further subdivided into four distinct α-helical coiled-coil segments (helix segments *1A*, *1B*, and *2A*, *2B*) with short, possibly nonhelical spacers between them (11, 19, 49, 50). The two polypeptide chains in the coiled-coil region of the molecule are parallel and in register (41, 44).

There is substantial sequence homology between different intermediate filament proteins (reviewed in references 11, 49, 50), particularly in the central rod region where, in addition to the heptad repeat characteristic of α-helical coiled-coils (12, 35), there is generally a series of zones of alternating positive and negative charge which repeats at $\sim$9.5 residue intervals or three times every 28 residues (11, 36). Although interactions between the globular NH_2- and COOH-terminal domains are probably also involved, an important source of interactions between these proteins in intermediate filaments in vivo is thought to involve complementation of the alternating bands of charge in the rod sections of adjacent

---

1. *Abbreviation used in this paper:* GFAP, glial fibrillary acidic protein.
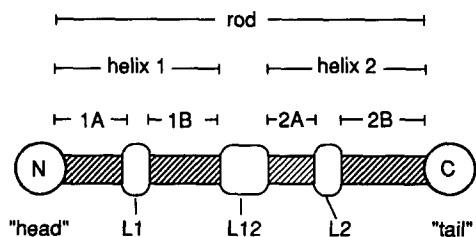
Figure 1. Schematic illustration of the general molecular structure of intermediate filament proteins suggested by Geisler and Weber (19). A central mainly α-helical coiled-coil rod $\sim$45–50 nm long is flanked by nonhelical regions, with that at the NH$_2$ terminus being referred to as the *head* and that at the COOH terminus as the *tail*. The rod is further subdivided into two main helical regions, 1 and 2, which are linked by a short region (*L12*), which probably does not have a coiled-coil conformation. Each helical region can be further subdivided, so that *helix 1* has domains *1A* and *1B* linked by *L1* (which may be nonhelical), whereas *L2* divides *helix 2* into domains *2A* and *2B*. There may also be a local disturbance to the coiled-coil structure in the COOH-terminal half of helix *2B* (the "stutter").

molecules. However, there must be interactions in addition to those between the rod portions, since proteolytic fragments corresponding to the rod domain do not assemble by themselves into filaments (19, 48). It seems likely that the nonhelical COOH-terminal "tail" domain of the molecule may be less important for intermediate filament formation than the nonhelical NH$_2$-terminal "head" (5, 30, 45).

Solution studies on a broad range of intermediate filament proteins and proteolytic fragments that correspond to the rod domain (3, 24, 44, 47, 49, 50, 57–59) have supported the concept that the two-chain molecules associate to form molecular dimers containing four chains, which are often referred to as "tetramers." It seems likely that analogous tetramers are also intermediates in filament assembly in vivo (6, 47). There has been some controversy about the precise molecular arrangement in the tetramers (see references 50, 51). Although the molecules appear to be antiparallel (21), electron microscopy (21, 28) has indicated an almost complete overlap, whereas particles isolated from cross-linked keratin filaments (16, 17, 59) indicate that the molecules in tetramers overlap by approximately half their length. Of course, within the actual intermediate filament, each molecule will interact with a number of nearest neighbors and so, in vivo, there will be a range of molecular interactions in addition to those seen in tetramers in solution (see references 16, 17).

In this article we describe the production of paracrystals of a 341–amino acid fragment of mouse GFAP that corresponds broadly to the α-helical coiled-coil rod segment of the molecule. We have established the relative positions of the molecules in a number of polymorphic forms of these paracrystals which enabled the types of molecular interaction between the rod molecules to be evaluated and related to interactions within tetramers and whole intermediate filaments.

Materials and Methods

Expression of GFAP Rod Fragment

A c-DNA fragment (obtained courtesy of Dr. N. Cowan, New York Univer-

sity Medical School) coding for the COOH-terminal 403–amino acid residues of mouse GFAP (32) was truncated at base 1,047 using oligonucleotide-directed site-specific mutagenesis in M13 and inserted into a modification of the expression vector pLcII (37) using standard recombinant DNA methods as described in detail by Quinlan et al. (45). As illustrated in Fig. 2, this vector produced a fusion protein containing the first 32 residues of the λ cII protein followed by a proteolysis site and then the GFAP protein fragment. The fusion protein was expressed in *Escherichia coli* (37) and isolated as inclusion bodies as described (45). The inclusion bodies were solubilized in 9.5 M urea, 5 mM EDTA, 10 mM Tris-HCl, 1% β-mercaptoethanol, pH 8, at room temperature, and renatured by two-stage dialysis procedure into 1% β-mercaptoethanol, 10 mM Tris-HCl, pH 8, at room temperature. The λ cII peptide was then removed by overnight cleavage with thrombin as described (45) to yield generally $\sim$5–10 mg of GFAP rod fragment per liter of culture medium. The fragment was purified by ion-exchange chromatography over Merck TSK DEAE-650(M) resin in 8 M urea, 5 mM EDTA, 2 mM DTT, 10 mM Tris, pH 8.5 at room temperature, using a 0–300-mM NaCl gradient, and was essentially homogeneous by SDS-PAGE (Fig. 3) as described (31). The fragment was then dialyzed against 10 mM Tris-acetate, pH 8.0, at 20°C in two stages and frozen until required.

Preparation of Paracrystals

Paracrystals were formed over a range of conditions and generally solutions of 0.5–3.5 g/liter of the GFAP rod fragment in 10 mM Tris-acetate, pH 8, at room temperature were made 0.25–0.5 M in KSCN and then divalent cation (Mg, Ca, or Ba as the acetate salt) added to the same concentration as thiocyanate. Best results seemed to be obtained at lower protein concentrations and $\sim$0.4 M thiocyanate and divalent cation, but there was, as is usual in this sort of system, some variation between runs. Paracrystals usually formed in minutes, producing a distinctly cloudy solution, although often best results were obtained with samples that had stood at room temperature for several hours. Samples for electron microscopy were prepared by floating carbon-coated 400-mesh grids on drops of paracrystal suspension followed by floating on drops of 1 or 2% aqueous uranyl acetate and air drying. Positively stained specimens were prepared by floating on several drops of demineralised water after uranyl acetate staining.
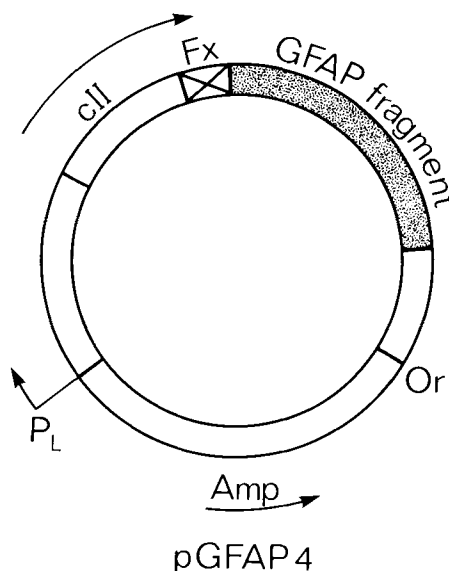

pGFAP4

Figure 2. Illustration of the plasmid construct, pGFAP4, that was used to express in *E. coli* an engineered c-DNA fragment corresponding to the mouse GFAP rod. The plasmid was based on the pLcII expression vector (32) and produced a fusion protein containing 32 residues of the λ cII protein, followed by a factor X (*Fx*) site and then the GFAP c-DNA fragment. Expression was under the control of the λ P$_L$ promotor using the cI[857] temperature-sensitive mutant. The construction of this plasmid is described in detail by Quinlan et al. (45).

Figure 3. SDS-PAGE patterns showing the purification of the protein fragment corresponding to the GFAP rod. (Lanes *1* and *6*) Molecular weight markers; (lane *2*) uninduced cells; (lane *3*) induced cells; (lane *4*) inclusion bodies; (lane *5*) the GFAP rod fragment after removal of the cII protein fragment with thrombin.

Electron Microscopy

Paracrystals were examined using Philips EM301, EM400, EM420, and CM12 electron microscopes operated at 80 kV generally with 0.03-mm objective apertures. Micrographs were recorded at nominal magnifications between 30,000 and 70,000 using Kodak SO-163 cut film. Magnification was calibrated using the 2.81-nm axial repeat of *Methanospirillum hungatei* sheaths negatively stained with uranyl acetate (54).

Results

Expression and Characterization of the GFAP Rod Fragment

We have described in detail elsewhere (45) the expression in *E. coli* of fragments of GFAP. In the present study, we used a fragment comprising residues 6 to 347 of the mouse GFAP amino acid sequence numbered according to Lewis et al. (32) which, by analogy with proteolysis studies of a range of intermediate filament proteins (19, 20, 30), broadly corresponded to the rod portion of GFAP. Although there seems to be general agreement that the COOH-terminal boundary of the rod corresponds to Ile-347, the NH$_2$-terminal boundary of the rod is less certain. The heptad repeat characteristic of a coiled-coil conformation does not begin until about residue 40, but digestion with chymotrypsin suggests that the coil may extend for a further 20 residues towards the NH$_2$-terminus (30). To ensure that we obtained the whole GFAP rod, we therefore chose to make a fragment that spanned from the endogenous thrombin site at Phe-6 to Ile-347. Con-

sequently, it is likely that the fragment we used for our studies contained a portion of the NH$_2$-terminal nonhelical domain in addition to the entire α-helical coiled-coil rod.

We have described elsewhere (45) the characterization of this expressed material using SDS-PAGE, Western blotting, and cross-linking to demonstrate that it corresponded to the expected portion of GFAP and that it retained the structural properties necessary for the formation of dimers and tetramers. Material sprayed onto mica and unidirectionally shadowed with platinum showed rod-shaped particles that had a bi-modal length distribution with maxima at 48 and 63 nm, which was similar to the length distribution seen with proteolytic fragments corresponding to the rod domain of desmin (30).

Paracrystals Formed with Divalent Cations

The classic studies of Cohen and her co-workers (7–10) have indicated that often paracrystals can be formed from fibrous proteins using divalent cations. We found that these methods were also effective with the expressed GFAP rod fragment and the addition of divalent cations such as Mg, Ca, Sr, Ba, and Mn, produced dense precipitates of paracrystals. However, these paracrystals were generally of rather limited extent and lacked clear axial banding patterns. Moreover, they were usually very tangled, which made it difficult to obtain clear views. A significant improvement resulted from adding a chaotrophic agent, which probably helped disperse the material. Thiocyanate, which was used previously by Cohen et al. (9) to produce paracrystals of myosin rod with divalent cations, seemed to be particularly effective in this respect and, as illustrated in Figs. 4 and 5, distinctive paracrystals were obtained in 0.25–0.5 M KSCN with Mg or Ba ions at the same concentration as thiocyanate. Generally, these patterns were only observed for pH values near 8. Below about pH 7.5 the paracrystals lacked clear axial banding patterns, whereas above pH 8.5 they tended to clump so severely that it was difficult to make out the precise nature of the pattern present.

The pattern in negatively stained paracrystals had an axial repeat of 57 nm (± 1 nm, $n = 11$) and was dominated by two dark zones ~ 11 nm wide, separated by a narrow light zone ~ 2–3 nm wide. The pattern had clear dyad symmetry, indicating an antiparallel arrangement of molecules in the unit cell. Broken paracrystals, paracrystals with blunt ends, and small paracrystal fragments were common (Figs. 4 and 5). In all of these, the pattern terminated at the narrow light band between the two dark bands in the axial repeat. This indicated that one end of the molecules in the paracrystal was located at this position in the axial repeat. In some instances a feint lightly staining band could be seen at the end of the broken paracrystal fringe which probably indicated a slight divergence from the coil-coil conformation in this region, analogous perhaps to that observed with tropomyosin (53). However, this band was much feinter than the band seen in this position in the interior of the paracrystals, which suggested that the narrow 2–3-nm-wide light zone in the staining pattern resulted, at least in part, from a superposition of molecules. In positively stained paracrystals (Fig. 6), the contrast of the pattern was essentially reversed, so that the two bands that had been dark in negatively stained material became light. This behavior indicated that the molecules were
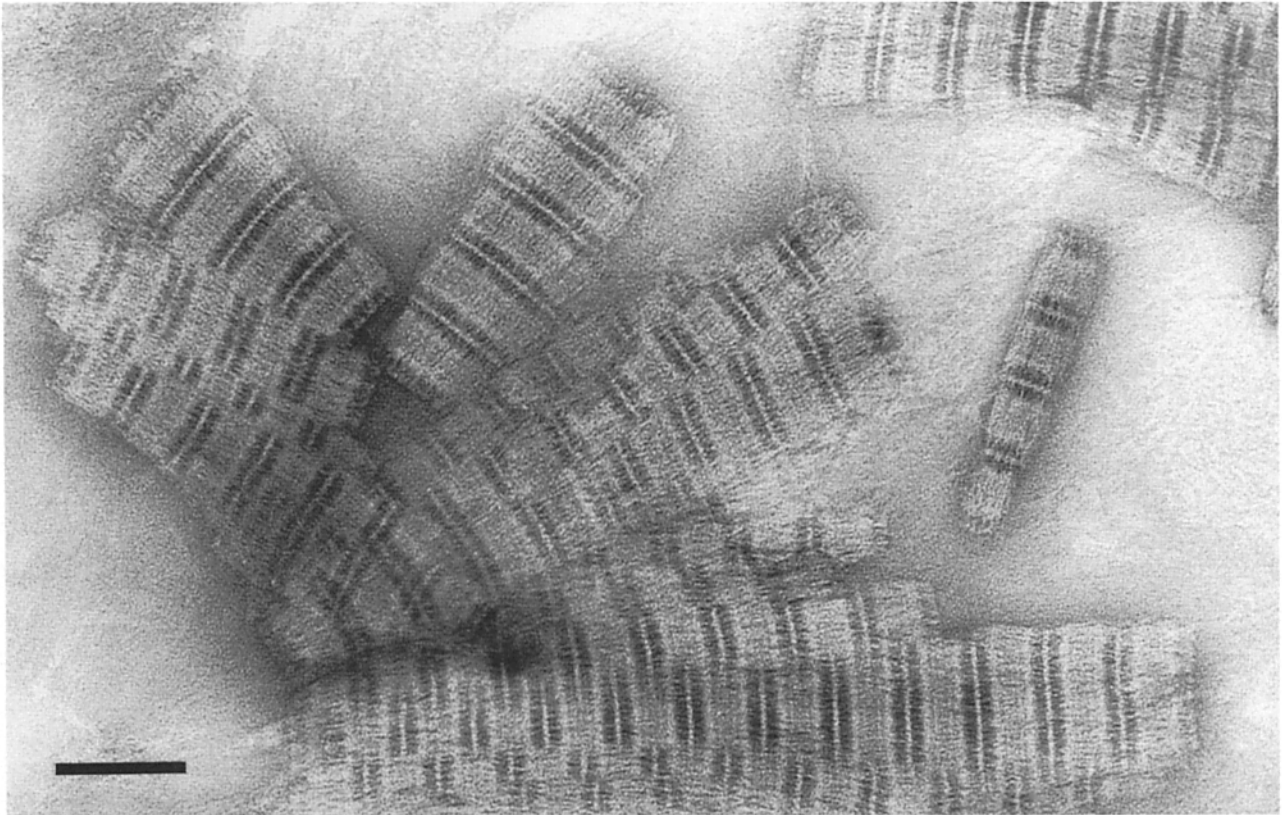
Figure 4. Magnesium paracrystals of the expressed protein corresponding to the rod portion of GFAP negatively stained with uranyl acetate. The paracrystals have a distinct banding pattern with a 57-nm axial repeat with dyad symmetry that contains two ∼11-nm-wide darkly staining bands separated alternately by thin, 2–3-nm-wide and thick, 34-nm-wide lightly staining bands. The ends of many paracrystals are blunt, with the pattern terminating at the narrow lightly staining band. Bar, 100 nm.
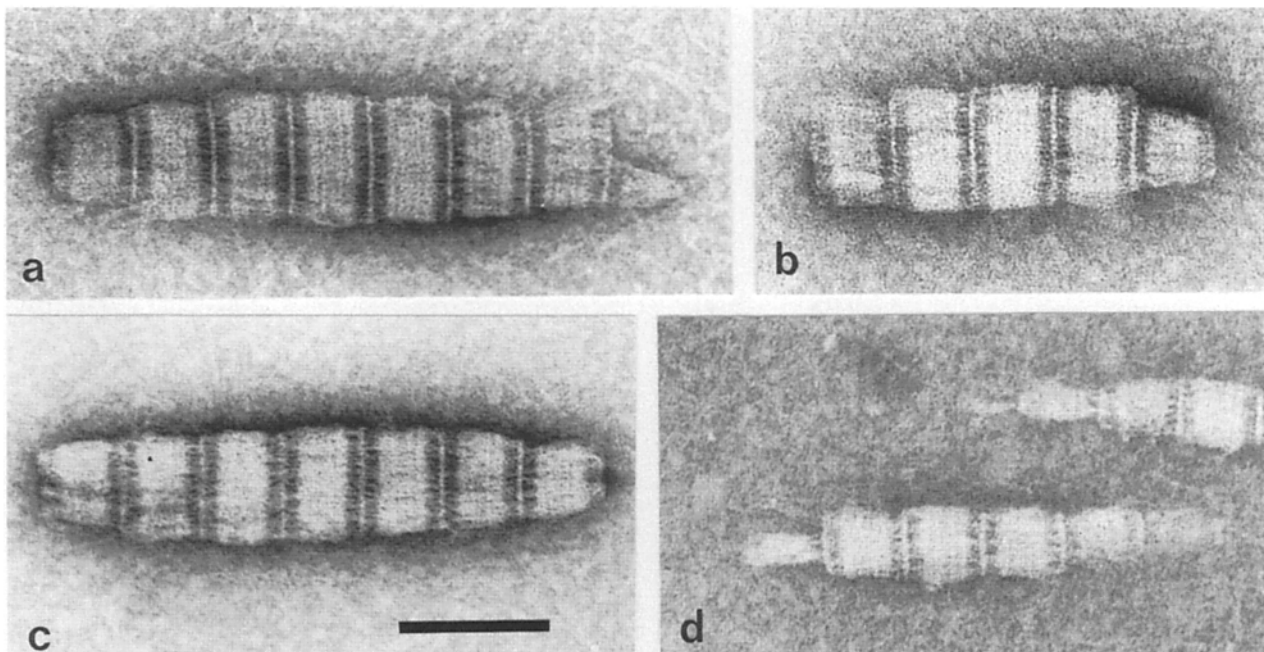

Figure 5. Barium paracrystals of GFAP rod negatively stained with uranyl acetate. The staining pattern is essentially the same as that seen with magnesium paracrystals. *a* and *d* show the termination of the pattern at the thin lightly staining band particularly clearly. Bar, 100 nm.
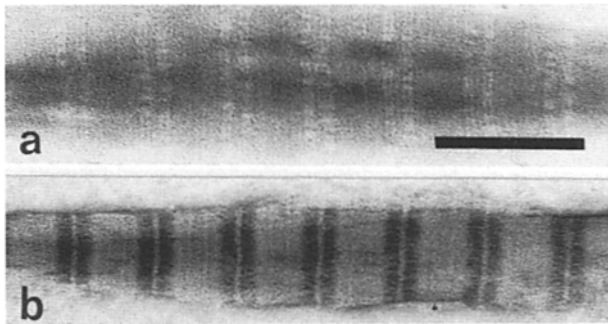
Figure 6. Comparison of the positive (*a*) and negative (*b*) staining patterns with barium paracrystals of the GFAP rod fragment. Although the contrast present in positively stained micrographs was much lower than in negatively stained ones, the prominent 11-nm-wide darkly staining bands seen with negative staining clearly has reversed contrast in the positively stained pattern. Bar, 100 nm.

arranged to produce a gap-overlap structure as discussed below.

In addition to the pattern resulting from the gap-overlap molecular arrangement in these paracrystals, there was also a fine pattern of bands with dyad symmetry that probably resulted mainly from specific attachment of the stain to groups in the protein sequence ("positive staining") that was analogous to that seen with other fibrous protein paracrystal patterns (7, 10, 53). Optical diffraction patterns from electron micrographs of negatively stained paracrystals (Fig. 7) showed a closely spaced pattern of meridional spots corresponding to the 57-nm axial repeat. Although some patterns showed a hint of row lines, sharp reflections characteristic of a two-dimensionally crystalline structure were not generally observed. However, often there was a broad diffuse equatorial reflection at ∼4 nm, which probably represented the average packing distance between molecules.

GFAP Rod-λ cII Fusion Protein Paracrystals

Paracrystals were also formed from the λ cII–GFAP rod fusion protein using the same conditions as were used with the isolated GFAP rod fragment, although these paracrystals generally seemed to be more tangled than those produced from the GFAP rod fragment, particularly when Ba was used as the precipitant. The negatively stained fusion protein paracrystals had a pattern that was analogous to that observed with the GFAP rod fragment, with a distinctive pattern of two closely spaced dark lines, separated by a thin white line, repeating axially every 57 nm (Fig. 8). However, the fusion protein paracrystals had two additional light bands in each axial repeat. These extra bands were located at the extremities of the long light band that separated the closely spaced dark bands (*arrows*, Fig. 8).

Polymorphism

In some instances, axial staining patterns were seen that derived from the superposition of axially staggered copies of the simplest (or fundamental) pattern. The basis of these patterns was easily confirmed by reference to the frequent aggregation of paracrystals side-by-side (Fig. 9). In these aggregates, the patterns of adjacent paracrystals were usually staggered by some fraction of the fundamental pattern period.

In one type, the adjacent patterns were staggered by half a repeat (Fig. 9, *d* and *e*), whereas in others a stagger of near 12 nm (Fig. 9 *a*) was seen, so that the narrow light band in one paracrystal was brought to lie next to the junction between the broad light band and a dark band in its neighbor. A stagger of ∼24 nm was also common (Fig. 9, *b* and *c*).

Discussion

Molecular Arrangement in the Paracrystals

The basic pattern seen in negatively stained preparations of the simplest paracyrstals of the expressed GFAP rod fragment consisted of two dark bands ∼11 nm wide separated by lighter bands alternatively ∼34- and 2–3-nm wide (Figs. 4 and 5). The contrast in this pattern was broadly reversed in positively stained material (Fig. 6), indicating that the dark bands in the negatively stained material resulted from stain penetration, suggesting a reduced protein density in this area. An analogous staining phenomenon has been observed in collagen (26) and in paramyosin paracrystals (10) and is indicative of a gap-overlap type of structure such as that illustrated in Fig. 10. In this structure, the unit cell consists of two antiparallel molecules that have two types of overlap: a long overlap, of ∼34 nm between one set of ends; and a short overlap, of ∼2–3 nm, between the other ends. The high protein density in both these regions would result in their appearing light in negatively stained material, whereas the lower protein density in the intervening regions would appear in darker contrast as a result of greater stain penetration. The molecules in the unit cell of this structure would be ∼48 nm long, which is in excellent agreement with
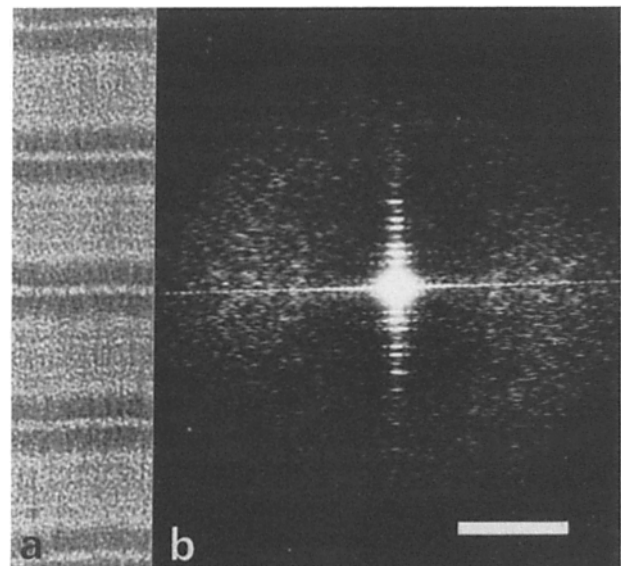

Figure 7. Optical diffraction pattern (*b*) from a micrograph of a GFAP rod fragment magnesium paracrystal negatively stained with uranyl acetate (*a*). Following the usual crystallographic convention, the pattern is oriented with the fiber axis vertical, and so axial repeats in the paracrystal produce the pattern of spots corresponding to orders of 57 nm along the meridian. In addition there are diffuse equatorial reflections at ∼4 nm that probably derive from the spacing between units across the paracrystal. Bar, 5 nm.
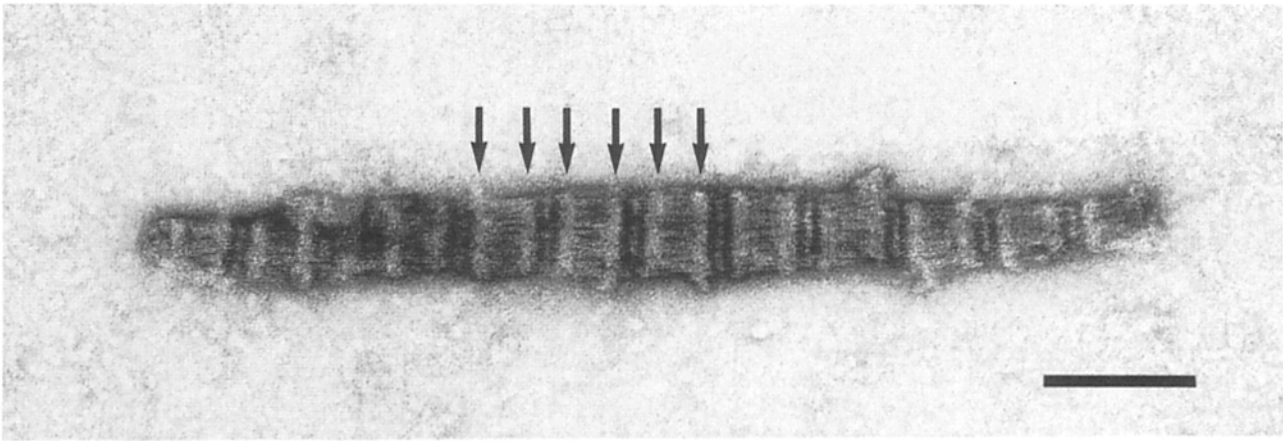
Figure 8. Paracrystals formed from the λ cII-GFAP rod fusion protein in 0.5 M Mg acetate, 0.5 M KSCN, 10 mM Tris-HCl, pH 8, negatively stained with uranyl acetate. When this pattern is compared to that in paracrystals derived from the GFAP rod fragment alone, there are two additional light bands per axial repeat, located at the extremities of the long light band joining the dark bands (*arrows*). These additional light bands correspond to the increased protein density associated with the λ cII fragment attached to the GFAP rod NH₂ terminus. Bar, 100 nm.

predictions based on the length of the sequence, with length determinations on other intermediate filament protein rods (19, 21, 27, 28, 44), and with the length measured for this material in unidirectionally shadowed preparations (45).

In paracrystals formed from the fusion peptide (in which 32 residues of the λ cII protein were added to the NH₂ terminus of the GFAP rod fragment) extra material was located at the edges of the broad light zone, immediately adjacent to the dark zones. This result identified the orientation of the molecules in these paracrystals and showed that the long overlap corresponded to that between the NH₂ termini of the fragment, whereas the short overlap involved a small region at the COOH termini. Thus, the major overlap between the two molecules in the unit cell involves the helix 1 regions of the molecule and it may be that the phase change in the 28/3 residue charged repeat associated with linker 12 (11) is an important determinant in limiting the overlap at this point (17). There are also two possible disruptions to the coiled-coil structure in helix 2 (L2 and the "stutter"; see reference 11) which would lie near to the NH₂ terminus of the second molecule in the unit cell and these may also have a role in determining the extent of the stagger between molecules.

The manner in which paracrystals aggregated side by side (and the corresponding polymorphic patterns produced) was analogous to the polymorphism observed with several other fibrous protein paracrystals, most notably those of paramyosin (10). This polymorphism indicated that, in addition to stacking laterally, the molecules within the unit cells had an additional series of preferred interactions, the most common of which involved axial staggers of ∼1/5, 2/5, and 1/2 the axial repeat distance. It is probably only coincidence that the molecules in paramyosin paracrystals (10) are also often staggered by 2/5 the axial repeat (which, with paramyosin is 72.5 nm). However, it is likely that many of the interactions seen in the polymorphic forms reflect interactions present in intermediate filaments in vivo in an analogous way to that proposed (10) for paramyosin in muscle thick filaments. Unfortunately the dyad symmetry of the GFAP paracrystals results in a degree of ambiguity in the precise molecular interac-

tions, because it is not clear which molecule in one unit cell interacts with the staggered unit cell. Thus, for example, a stagger of 2/5 the axial repeat could result from either parallel or antiparallel molecules staggered by 24 nm. However, the number of possibilities is not very large and so these three observed staggers may serve as useful constraints on models of the molecular packing in intermediate filaments.

Implications for Molecular Arrangement in Tetramers

The simplest molecular arrangement in the basic paracrystals formed with divalent cations has two molecules arranged in an antiparallel manner in the unit cell. Since intermediate filament proteins and proteolytic fragments corresponding to the rod domain are known to form tetramers in solution (3, 24, 40, 47, 49, 50, 57-59), it seems very likely that the two molecules in the paracrystal unit cell correspond to the two molecules in "tetramers" that existed in solution before the addition of divalent cation. In this case, the role of the divalent cation would be to precipitate preexisting tetramers into paracrystals. An analogous condensation of molecular dimers is thought to be involved in the formation of myosin aggregates, such as muscle thick filaments (see reference 13). However, there may be a number of different tetramer arrangements in solution at any one time. This is a consequence of the repeating nature of the charge zone motif (see reference 11) so that complementation of charges can occur for any stagger between molecules that corresponds to an odd number of half-repeats. A range of molecular dimers are thought to exist for myosin in solution (46) and the presence of more than one vimentin tetramer has been proposed (40). Therefore precipitation with divalent cations may select only one tetramer arrangement from a range present in solution. Moreover, the different molecular staggers observed in the polymorphic forms would be consistent with other tetramer interaction geometries which were either not so common in solution as the geometry selected in the unit cell of the basic paracrystal pattern or which, perhaps, were not selected as effectively by the divalent cations used to form the paracrystals. However, as we discuss below, the molecular arrange-
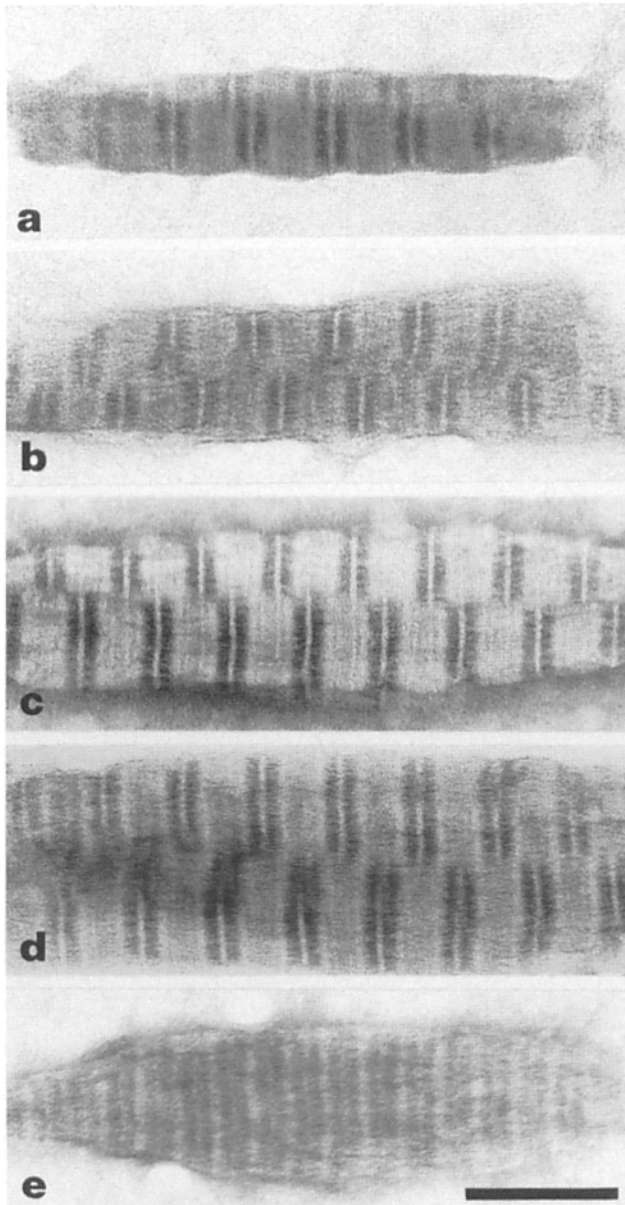
Figure 9. Polymorphic forms and aggregates of paracrystals of GFAP rod negatively stained with uranyl acetate. (*a*) Magnesium paracrystal showing a stagger of 1/5 the axial repeat (12 nm) so that the fine light band in one repeat is opposite the junction between the long light band and the dark band in the other; magnesium (*b*) and barium (*c*) paracrystals showing a stagger of 2/5 the axial repeat (∼24 nm) so that junctions between the dark bands and the long light band are opposite one another. *d* shows a magnesium paracrystal staggered by ½ the axial repeat and *e* shows the pattern produced by this superposition. Bar, 100 nm.

ment within the unit cell of the paracrystals is consistent with data from other sources which indicates that it is probably closely related to the molecular packing in intermediate filaments in vivo. In particular, the observation of a number of different interaction geometries between molecules probably accurately mirrors the arrangement within intermediate filaments where each molecule probably interacts with several different nearest neighbors as a consequence of the molecules overlapping along their length.

The molecular interaction geometry in the paracrystal unit cell is consistent with some other data on the molecular arrangement within tetramers. For example, partial digestion of wool gives a 1B tetramer (3, 24, 57–59) which would be consistent with an antiparallel overlap of ∼1/2 molecular length. Electron micrographs of shadowed tetramers to which a monoclonal antibody was bound to a region near the COOH-terminal region of the rod showed that the antibody molecules were ∼45 nm apart (21). On this basis, it was proposed that the molecules in this antiparallel tetramer overlapped almost completely (21). However, since the epitope recognized by the antibody was only confined to between residue 324 and 415 (21), a considerable range of molecular staggers would be consistent with this result. If one takes the unit axial rise in an α-helical coiled-coil as 0.15 nm (14), our model for the tetramer (Fig. 10) would predict spacings between antibody-binding sites of ∼30–60 nm (depending on where the epitope was located along the rod between residues 324 and 415) and so would be consistent with the 45-nm separation observed (21).

The molecular arrangement in the paracrystal unit cell is not consistent with some electron microscopy results obtained with keratin and desmin (28, 43). With desmin, 48-nm-long particles were seen (28) under conditions which earlier studies (55) had indicated that the material was present as "protofilaments," which were identified with molecular dimers (i.e., "tetramers"). On this basis, a tetramer model was proposed in which the molecules ("dimers") overlapped by essentially their entire length (28). Particles 70 nm long were also observed when the salt concentration was raised and were proposed to be octamers in which two tetramers were staggered by 24 nm (28). However, the state of aggregation of intermediate filament proteins under the precise conditions used to prepare specimens for electron microscopy does not appear to have been thoroughly characterized. It is conceivable that, under these conditions and at the high dilutions usually used, the tetramers had dissociated into dimers and so the 48-nm rods observed corresponded to single molecules and the 70-nm rods corresponded to tetramers. This interpretation would be more consistent with the molecular positions we found in paracrystals. Alternatively, it could be that in the different conditions and with the different proteins we and Ip et al. (28) used, different tetramers were formed or possibly more than one type of tetramer was present (40). The desmin results do, however, raise the question that the unit cell in the paracrystals might not contain two molecules but rather four, since, if two tetramers in which the molecules overlapped almost completely were staggered by ∼34 nm, a pattern very similar to the one we observed would be produced. We think this is not likely to be the correct interpretation, because the results with the fusion protein indicated that extra material was present only at the ends of the long light band. This was the result expected if there were only two molecules in the unit cell, whereas, if there were four molecules in the unit cell, extra material should also have been seen at the fine light band. Moreover, the broad equatorial reflection at ∼4 nm in optical diffraction patterns of micrographs of negatively stained material would suggest that the centers of units within the paracrystals were spaced ∼4 nm apart laterally. However, the broad nature of the reflection indicated that this was only an average value and that spacings both above and below this value were present.
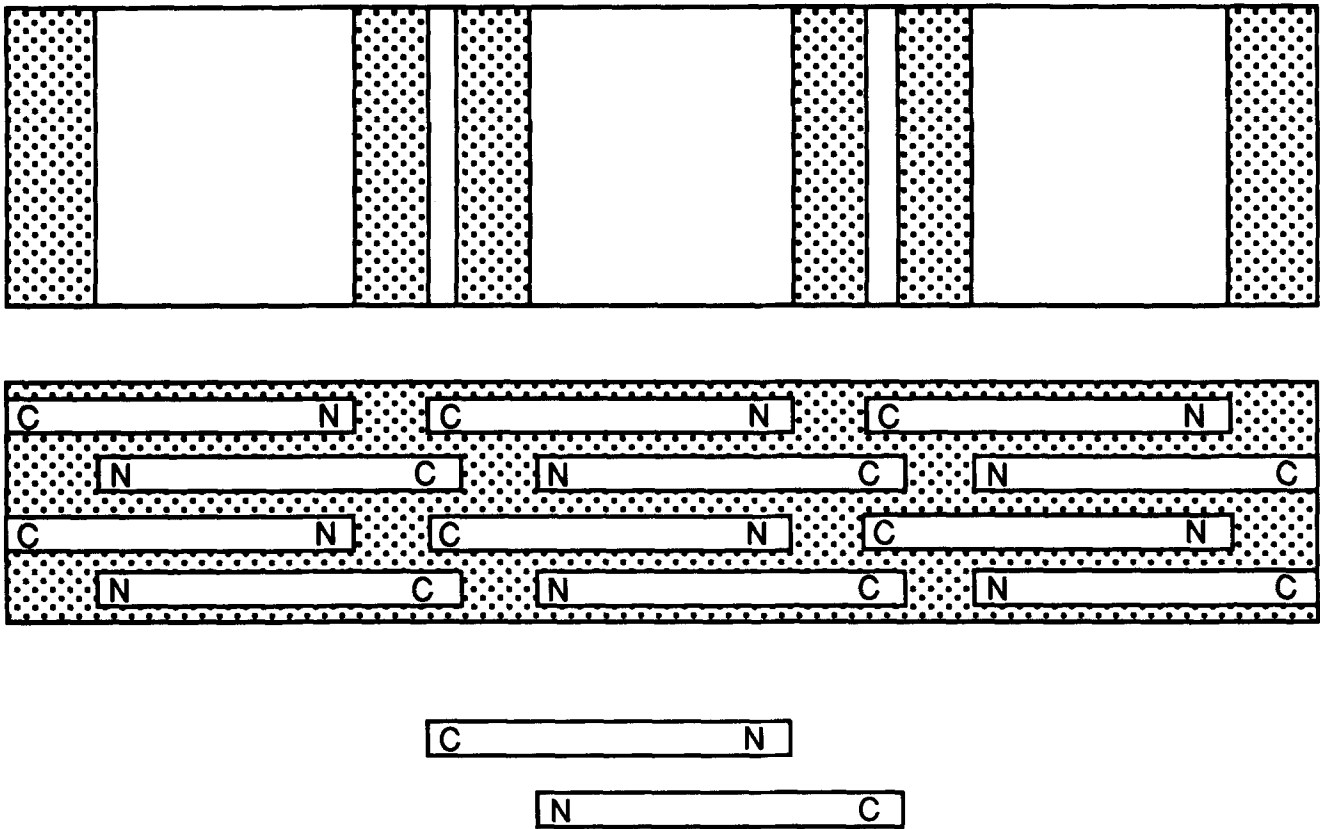
Figure 10. Schematic representation of the molecular arrangement in the fundamental pattern observed in paracrystals of GFAP rod. The molecules in the unit cell are arranged so that their NH_2 termini overlap by $\sim$34 nm and their COOH termini overlap by $\sim$2–3 nm. The protein density in the overlap regions is double that in the intervening region and so the two overlap regions appear light in negative stain and the intervening regions dark.

On this basis it would appear likely that the actual width of the basic packing units was probably somewhat <4 nm, which would be more consistent with their being tetramers, since octamers would probably be wider than 4 nm (see reference 1). Implicit in this discussion has been the assumption of an antiparallel arrangement of molecules within the tetramer as suggested strongly by the results of Geisler et al. (21). If the molecules within tetramers were arranged parallel to one another, then, in an octamer constructed from two antiparallel tetramers, both the staining pattern and location of the additional cII material would be similar to that we observed. Although we cannot unequivocally rule out such an interpretation of the molecular arrangement in the unit cell, the results of Geisler et al. (21) and the probable width of packing units in the paracrystal would seem to make it unlikely.

Others (2, 23, 60) have reported the formation of paracrystals from lamins and one of these has been analyzed (39) to attempt to establish molecular positions. Unfortunately the axial repeat of the lamin paracrystals was less than the molecular length, and so the consequent overlapping of molecules made it difficult to establish molecular positions unequivocally. However, it seemed fairly certain, based on a range of modelling studies and computer analyses of likely interactions between molecules, that the unit cell contained four lamin molecules arranged in two antiparallel pairs that overlapped by about half their length (39). One common feature of these models for lamin paracrystal structure was a

strong interaction between helix 1A and the strongly conserved COOH-terminal region of helix 2 in parallel molecules. Because there was still some ambiguity about the way in which the lamin molecules were paired, it was not possible to say how precisely some aspects of the molecular packing in the paracrystals may resemble the geometry we have established for the recombinant GFAP fragment paracrystals, although in the GFAP paracrystals we instead observed strong interactions between the helix 2 COOH termini in antiparallel molecules (see Fig. 10).

Implications for Intermediate Filament Structure

Fraser and his colleagues have made a very detailed examination of the molecular arrangement in intermediate filaments derived from hard mammalian keratins such as wool, horn, and quills (see references 15, 16) and have investigated (17) possible molecular arrangements that would be consistent with both x-ray diffraction data on the symmetry of the filaments and also with maximizing ionic interactions between molecules. From this study they derived a number of plausible models, one of which was shown in Fig. 8 c of reference 17 and which, moreover, appeared to be more consistent with the available data than any of their other models (16). In this model there were four interactions between intermediate filament molecules and it is intriguing that two of these (between almost completely overlapping antiparallel helix 1B segments and between short regions at the COOH

termini of antiparallel helix 2 segments) were those seen in the GFAP rod paracrystals. In the Fraser et al. (17) model these interactions were found between tetramers lying essentially side-by-side, whereas in the paracrystals the interactions are between tetramers joined end-to-end and this may account for the different structures formed in each instance. The different polymorphic paracrystalline forms observed with the GFAP fragment indicated the presence of additional interactions between the tetramers that may be related to filament formation, but none of these interactions seemed to be paralleled closely by the Fraser et al. (17) models. Of course, it could be that these ideally helical models may not be strictly correct as there is evidence that many intermediate filaments are constructed from probably four subfilaments (1), although the appearance of subfilaments might perhaps be a reflection of the different interactions between molecules in the filament (16).

There have been several indications of a 22-24-nm axial periodicity in intermediate filaments (25, 29, 33) which may derive from either the axial stagger of molecules within the filament or perhaps from some aspects of the helical symmetry of the filament (see reference 17). In this context it is perhaps intriguing that the 2/5 stagger between unit cells seen in some of the polymorphic paracrystalline forms (Fig. 9, b and c) is close to 24 nm and so may represent the molecular interaction that gives rise to the periodicity observed in intact filaments. However, in addition to the interactions between the rod portions of the molecule, intermediate filaments probably also require specific interactions between the nonhelical head and tail portions of the molecule (see references 19, 30, 45, 48) which will not be manifest in the paracrystals we have discussed in this manuscript. We have prepared a range of different fragments of GFAP to help address the role of the nonhelical domains (45) but to date we have succeeded in forming paracrystals only from the fragment corresponding to the rod domain.

In addition to the correspondence between the molecular positions in the divalent cation-induced GFAP rod paracrystals and those predicted by the keratin structural model (17), there are other indications that the molecular interactions observed in the paracrystals probably corresponded to those in filaments. The strong interactions that we observed between short stretches of the COOH terminus of the GFAP rod are in a region that is strongly conserved between intermediate filament sequences (see references 11, 18) which suggests that they may have an important role in the structure and assembly of intermediate filaments. This concept is reinforced by the observation (4) that, in cultured epidermal cells, deletions of the COOH terminus of a cytokeratin did not influence its assembly and integration into existing intermediate filaments until the deletion included a small portion of the COOH terminus of the rod domain. Moreover, the strong interactions between antiparallel helix 1B domains present in the paracrystals were consistent with proteolysis studies of wool keratins that indicated a strong interaction between these regions of the molecules (24, 58).

Some recent work has indicated that intermediate filaments may attach to specific sites on the nuclear and plasma membranes and have a vectorial assembly mechanism (22, 56). Clearly one way in which vectorial assembly could be generated would be by the filaments possessing an underlying polarity, which would not be consistent with an an-tiparallel molecular packing. But vectorial assembly could also result from the attachment at different cellular sites depending on different domains in the intermediate filament proteins, in which case either parallel or antiparallel molecular packing within intermediate filaments would be possible. There is indeed evidence that attachment at different cellular sites does involve different portions of vimentin (22) and it would appear likely that these filaments initially attach near the nuclear envelope by their COOH-terminal domain and then extend into the cell cortex where they may attach to the plasma membrane (22, 56). Thus it would appear that an antiparallel molecular packing in the tetramer is not inconsistent with the vectorial assembly of intermediate filaments.

The close parallel between the molecular interactions seen in these paracrystals and those in intermediate filaments indicate that the paracrystals will be a useful model system for exploring these interactions in greater detail. We are currently doing this using oligonucleotide-directed site-specific mutagenesis and are also attempting to grow better crystals similar to those obtained for a myosin rod fragment (42) to determine molecular parameters such as the coiled-coil pitch.

References

1. Aebi, U., W. F. Fowler, P. Rew, T.-T. Sun. 1983. The fibrillar structure of keratin filaments unravelled. *J. Cell Biol.* 97:1131-1143.
2. Aebi, U., J. Cohn, L. E. Buhle, and L. Gerace. 1986. The nuclear lamina is a meshwork of intermediate-type filaments. *Nature (Lond.).* 323:560-564.
3. Ahmadi, B., and P. T. Speakman. 1978. Suberimidate crosslinking shows that a rod-shaped low-cysteine high-helix protein prepared by limited proteolysis of reduced wool has four protein chains. *FEBS (Fed. Eur. Biochem. Soc.) Lett.* 94:365-367.
4. Albers, K., and E. Fuchs. 1987. The expression of mutant epidermal keratin cDNAs transfected in simple epithelial and squamous cell carcinoma lines. *J. Cell Biol.* 105:791-806.
5. Bader, B. L., T. M. Magin, M. Hatzfeld, and W. W. Franke. 1986. Amino acid sequence and gene organisation of cytokeratin no. 19, an exceptional tail-less intermediate filament protein. *EMBO (Eur. Mol. Biol. Organ.) J.* 5:1865-1875.
6. Blikstad, I., and E. Lazarides. 1983. Vimentin filaments are assembled from a soluble precursor in avian erythroid cells. *J. Cell Biol.* 96:1803-1808.
7. Caspar, D. L. D., C. Cohen, and W. Longley. 1969. Tropomyosin crystal structure, polymorphism and molecular interactions. *J. Mol. Biol.* 41:87-101.
8. Cohen, C., and W. Longley. 1966. Tropomyosin paracrystals formed with divalent cations. *Science (Wash. DC).* 152:794-796.
9. Cohen, C., S. Lowey, R. G. Harrison, J. Kendrick-Jones, and A. G. Szent-Györgyi. 1970. Segments from myosin rods. *J. Mol. Biol.* 47:605-609.
10. Cohen, C., A. G. Szent-Györgyi, and J. Kendrick-Jones. 1971. Paramyosin and the filaments of molluscan catch muscle. 1. Paramyosin structure and assembly. *J. Mol. Biol.* 56:223-237.
11. Conway, J. F., and D. A. D. Parry. 1988. Intermediate filament structure: 3. Analysis of sequence homologies. *Int. J. Biol. Macromol.* 10:79-98.
12. Crick, F. H. C. 1953. The packing of α-helices: simple coiled-coils. *Acta Crystallogr.* 6:689-697.
13. Davis, J. 1988. Assembly processes in vertebrate skeletal thick filament formation. *Annu. Rev. Biophys. Biophys. Chem.* 17:217-239.
14. Fraser, R. D. B., and T. P. MacRae. 1973. Conformation in Fibrous Proteins. Academic Press Inc., New York. 628 pp.
15. Fraser, R. D. B., and T. P. MacRae. 1985. Intermediate filament structure. *Biosci. Rep.* 5:573-579.
16. Fraser, R. D. B., and T. P. MacRae. 1988. Surface lattice in α-keratin filaments. *Int. J. Biol. Macromol.* 10:178-184.

17. Fraser, R. D. B., T. P. MacRae, E. Suzuki, and D. A. D. Parry. 1985. Intermediate filament structure: 2. Molecular interactions in the filament. *Int. J. Biol. Macromol.* 7:258-274.

18. Geisler, N., and K. Weber. 1982. Related amino acid sequences in neurofilament and non-neuronal intermediate filaments. *Nature (Lond.).* 296:448-450.

19. Geisler, N., and K. Weber. 1982. The amino acid sequence of chicken muscle desmin provides a common structural model for intermediate filament proteins. *EMBO (Eur. Mol. Biol. Organ.) J.* 1:1649-1656.

20. Geisler, N., E. Kaufmann, and K. Weber. 1982. Proteinchemical characterisation of three structurally distinct domains along the protofilament unit of desmin 10 nm filaments. *Cell.* 30:277-286.

21. Geisler, N., E. Kaufmann, and K. Weber. 1985. Antiparallel orientation of the two double-stranded coiled-coils in the tetrameric protofilament unit of intermediate filaments. *J. Mol. Biol.* 182:173-177.

22. Georgatos, S. D., and G. Blobel. 1987. Two distinct attachment sites for vimentin along the plasma membrane and nuclear envelope in Avian erythrocytes: a basis for a vectorial assembly of intermediate filaments. *J. Cell Biol.* 105:105-115.

23. Goldman, A. E., G. Maul, P. M. Steinert, H. Y. Yang, and R. D. Goldman. 1986. Keratin-like proteins that coisolate with intermediate filaments in BHK-21 cells are nuclear lamins. *Proc. Natl. Acad. Sci. USA.* 83:3839-3844.

24. Gruen, L. C., and E. F. Woods. 1983. Structural studies on the microfibrillar proteins of wool. *Biochem. J.* 209:587-595.

25. Henderson, D., N. Geisler, and K. Weber. 1982. A periodic ultrastructure in intermediate filaments. *J. Mol. Biol.* 155:173-176.

26. Hodge, A. J., and J. A. Petruska. 1963. Recent studies with the electron microscope on ordered aggregates of tropocollagen. *In* Aspects of Protein Structure. G. N. Ramachandran, editor. Academic Press Inc., New York. 289-300.

27. Ip, W. Modulation of desmin intermediate filament assembly by a monoclonal antibody. *J. Cell Biol.* 106:735-745.

28. Ip, W., M. K. Hartzer, Y. Y. S. Pang, and R. M. Robson. 1985. Assembly of vimentin and its implications concerning the structure of intermediate filaments. *J. Mol. Biol.* 183:365-375.

29. Kallman, F., and N. K. Wessels. 1967. Periodic repeat units of epithelial cell tonofilaments. *J. Cell Biol.* 32:227-231.

30. Kaufmann, E., K. Weber, and N. Geisler. 1985. Intermediate filament forming ability of desmin derivatives lacking either the amino-terminal 67 or the carboxyl-terminal 27 residues. *J. Mol. Biol.* 185:733-742.

31. Laemmli, U. K. 1970. Cleavage of structural proteins during the assembly of the head of bacteriophage T4. *Nature (Lond.).* 227:680-685.

32. Lewis, S. A., J. M. Balcarek, V. Krek, M. Shelanski, and N. J. Cowan. 1984. Sequence of a cDNA clone encoding mouse glial fibrillary acidic protein: structural conservation of intermediate filaments. *Proc. Natl. Acad. Sci. USA.* 81:2743-2746.

33. Milam, L., and H. P. Erickson. 1982. Visualization of a 21-nm axial periodicity in shadowed keratin filaments and neurofilaments. *J. Cell Biol.* 94:592-596.

34. Moll, R., W. W. Franke, D. L. Schiller, B. Geiger, and R. Krepler. 1982. The catalogue of human cytokeratins: patterns of expression in normal epithelia, tumors and cultured cells. *Cell.* 31:11-24.

35. McLachlan, A. D., and M. Stewart. 1975. Tropomyosin coiled-coil interactions. *J. Mol. Biol.* 97:293-304.

36. McLachlan, A. D., and M. Stewart. 1982. Periodic charge distribution in the intermediate filament proteins desmin and vimentin. *J. Mol. Biol.* 162:693-698.

37. Nagai, K., and H.-C. Thøgersen. 1987. Synthesis and sequence-specific proteolysis of hybrid proteins produced in *Escherichia coli. Methods Enzymol.* 153:461-481.

38. Osborn, M., and K. Weber. 1986. Intermediate filament proteins: a multigene family distinguishing major cell lineages. *Trends Biol. Sci.* 11:469-472.

39. Parry, D. A. D., J. F. Conway, A. E. Goldman, R. D. Goldman, and P. M. Steinert. 1987. Nuclear lamin proteins: common structures for paracrystalline, filamentous and lattice forms. *Int. J. Biol. Macromol.* 9:137-145.

40. Potschka, M. 1986. Structure of intermediate filaments. *Biophys. J.* 49:129-130.

41. Quinlan, R. A., and W. W. Franke. 1982. Heteropolomer filaments of vimentin and desmin in vascular smooth muscle tissue and cultured baby hamster kidney cells demonstrated by chemical crosslinking. *Proc. Natl. Acad. Sci. USA.* 79:3452-3456.

42. Quinlan, R. A., and M. Stewart. 1987. Crystalline tubes of myosin long subfragment-2 that show the coiled-coil pitch and molecular interaction geometry. *J. Cell Biol.* 105:403-415.

43. Quinlan, R. A., J. A. Cohlberg, D. L. Schiller, M. Hatzfeld, and W. W. Franke. 1984. Heterotypic tetramer (A_2D_2) complexes of non-epidermal keratins isolated from rat hepatocytes and hepatoma cells. *J. Mol. Biol.* 178:365-388.

44. Quinlan, R. A., M. Hatzfeld, W. W. Franke, A. Lustig, T. Schulthess, and J. Engel. 1986. Characterisation of dimer subunits of intermediate filament proteins. *J. Mol. Biol.* 192:337-349.

45. Quinlan, R. A., R. D. Moir, and M. Stewart. 1989. Expression in *E. coli* of fragments of glial fibrillary acidic protein: characterisation, assembly and paracrystal formation. *J. Cell Sci.* 93:71-83.

46. Reisler, E., M. Burke, R. Josephs, and W. F. Harrington. 1973. Crosslinking of myosin and myosin filaments. *J. Mechanochem. Cell Motil.* 2:163-179.

47. Soellner, P., R. A. Quinlan, and W. W. Franke. 1985. Identification of a distinct soluble subunit of an intermediate filament protein: tetrameric vimentin from living cells. *Proc. Natl. Acad. Sci. USA.* 82:7929-7933.

48. Steinert, P. M. 1978. Structure of the three-chain unit of the bovine epidermal keratin filament. *J. Mol. Biol.* 123:49-70.

49. Steinert, P. M., and D. A. D. Parry. 1985. Intermediate filaments: conformity and diversity of expression and structure. *Annu. Rev. Cell Biol.* 1:41-65.

50. Steinert, P. M., and D. R. Roop. 1988. The molecular and cellular biology of intermediate filaments. *Annu. Rev. Biochem.* 57:593-625.

51. Steinert, P. M., and A. C. Steven. 1985. Splitting hairs and other intermediate filaments. *Nature (Lond.).* 316:767.

52. Steinert, P. M., A. C. Steven, and D. R. Roop. 1985. The molecular biology of intermediate filaments. *Cell.* 42:411-419.

53. Stewart, M. 1981. Structure of α-tropomyosin magnesium paracrystals II. Simulation of staining patterns and some observations on the mechanism of positive staining. *J. Mol. Biol.* 148:411-425.

54. Stewart, M., T. J. Beveridge, and G. D. Sprott. 1985. Crystalline order to high resolution in the shaft of *Methanospirillum hungatei*: a cross-β structure. *J. Mol. Biol.* 183:509-516.

55. Stromer, M. H., T. W. Huiatt, F. L. Richardson, and R. M. Robson. 1981. Disassembly of synthetic 10-nm desmin filaments from smooth muscle into protofilaments. *Eur. J. Cell Biol.* 25:136-143.

56. Vikstrom, K. L., G. G. Borisy, and R. D. Goldman. 1989. Dynamic aspects of intermediate filament networks in BHK-21 cells. *Proc. Natl. Acad. Sci. USA.* 86:549-553.

57. Woods, E. F. 1983. The number of polypeptide chains in the rod domain of bovine epidermal keratin. *Biochem. Int.* 7:769-774.

58. Woods, E. F., and C. Gruen. 1981. Structural studies on the microfibrillar proteins of wool: characterisation of the α-helix rich particle produced by chymotryptic digestion. *Aust. J. Biol. Sci.* 34:515-526.

59. Woods, E. F., and A. S. Inglis. 1984. Organisation of the coiled-coils in the wool microfibril. *Int. J. Biol. Macromol.* 6:277-283.

60. Zackroff, R. V., A. E. Goldman, J. C. R. Jones, P. M. Steinert, and R. D. Goldman. 1984. Isolation and characterisation of keratin-like proteins from cultured cells with fibroblastic morphology. *J. Cell Biol.* 98:1231-1237.